

PAPER • OPEN ACCESS

CFD Study of the effects of ingested bodies on the RSI of hydraulic turbines

To cite this article: A Guardo *et al* 2019 *IOP Conf. Ser.: Earth Environ. Sci.* **240** 022063

View the [article online](#) for updates and enhancements.

CFD Study of the effects of ingested bodies on the RSI of hydraulic turbines

A Guardo, A Fontanals, C Valero and E Egusquiza

Centre de Diagnostic Industrial i Fluidodinàmica, Universitat Politècnica de Catalunya BarcelonaTECH (UPC-CDIF), Av. Diagonal, 647, 08028, Barcelona, Spain.

Abstract. The ingestion of large bodies in hydraulic turbines can produce blockage in the runner and/or the distributor, modifying the amplitude and uniformity of pressure pulsations and generating large unbalanced forces. These unwanted effects can lead to reduced efficiency and increased vibration levels, which can produce significant mechanical damage. In this work, we present a characterization of the effects of flow blockages due to ingested bodies on the rotor-stator interaction (RSI) of hydraulic turbines by means of computational fluid dynamics (CFD). For this, a reduced-scale model of a pump turbine was implemented using Ansys® CFX v16.2, and numerical simulations were run for normal operation and blockage operation. Studied blockages included rotor and distributor blockages. Pressure pulsations in rotor and distributor were recorded in order to characterize the effect of the blockage on the RSI of the machine.

1. Introduction

Hydraulic turbines are a fundamental part of the power generation sector. Their capacity to rapidly supply power to the electrical grid during peak consumption hours makes them important in terms of grid stabilization. The reliability of these machines depends on their capacity to start up at any moment, their efficiency predictability and the avoidance of unexpected stops.

In general, large hydraulic turbines (except for high head turbines) are low rotating speed, rigid-shaft machines with low vibrating levels and reduced failure rates. Several studies have focused on the detection of mechanical damage [e.g. 1-3] or cavitation [e.g. 4-5] in these machines. However, in some cases, damage is generated by the ingestion of external bodies, rather than by failures in the machine itself. Hydraulic turbines suck in large amounts of water that can transport small particles, such as sand, and large bodies, such as large stones and logs. A body carried in the water will cause direct damage through impact or erosion and indirect damage through blockage [6].

If the ingested bodies are large enough (probably due to trash rack failure), they can cause the blockage of the runner or the distributor channels (see Figure 1). These blockages create unbalanced radial forces that increase the hydraulic excitation on the machine, thus they need to be detected before other parts of the machine suffer severe damage due to the increased vibration levels produced by these unbalances.

In this work, we present a characterization of the effects of flow blockages due to ingested bodies on the rotor-stator interaction (RSI) of hydraulic turbines by means of computational fluid dynamics (CFD). For this, a reduced-scale model of a pump turbine was implemented using Ansys® CFX v16.2, and numerical simulations were run for normal operation and blockage operation. Studied blockages



included rotor and distributor blockages. Pressure pulsations in rotor and distributor were recorded in order to characterize the effect of the blockage on the RSI of the machine.



Figure 1. Typical blockage on a turbine runner (left) or distributor (right) [6].

2. Methodology

2.1. Case study

The case study is a pump turbine turbine model ($D = 500$ mm) consisting of a runner with $z_b = 7$ blades and a distributor with $z_v = 16$ guide and stay vanes, rotating at $N = 600$ rpm. For this case, the runner rotation frequency is $f_f = 10$ Hz, the rotor blades frequency is $f_b = 70$ Hz (observed in the inertial reference frame), and the distributor vanes frequency is $f_v = 160$ Hz (observed in the rotating reference frame). These frequencies are determined from equations (1-3) (being n an arbitrary integer) [7]:

$$f_f = \frac{N}{60} \quad (1)$$

$$f_b = n \cdot f_f \cdot z_b \quad (2)$$

$$f_v = n \cdot f_f \cdot z_v \quad (3)$$

The computational model generated consisted of three control volumes (distributor, rotor and draft tube) united by numerical interfaces (Figure 2). Both unobstructed and obstructed cases were created for the rotor and the distributor control volumes. For the obstructed rotor case, a partial blockage (25, 50 and 75% canal blockage) was imposed in a rotor canal. For the obstructed distributor case partial (50%) and total (100%) blockage was imposed in a distributor canal.

2.2. Numerical procedure

Unsteady state numerical simulations were carried out using Ansys® CFX v16.2 CFD software, which simultaneously solves continuity and Navier-Stokes equation for a fluid in motion. SST $k-\omega$ turbulence model [8] was used to compute for the flow turbulent quantities. High-resolution schemes were used both for spatial and temporal discretization. The boundary conditions imposed consisted of

rotor rotational speed, flow rate and direction at the distributor inlet and atmospheric pressure at the draft tube outlet. Time step selected for the unsteady analysis corresponded to a 1° rotation of the runner. A sliding mesh approach was used in all simulations.

In order to record the RSI pressure pulsation five monitoring points were set in the numerical model (Figure 2): two monitoring points in the distributor at each side of a stay vane, and three monitoring points in the rotor located in the center of a canal at $0,8D$, $0,6D$ and $0,4D$. The temporal signals obtained were processed using a Fast Fourier transform (FFT) to represent the results in the frequency domain.

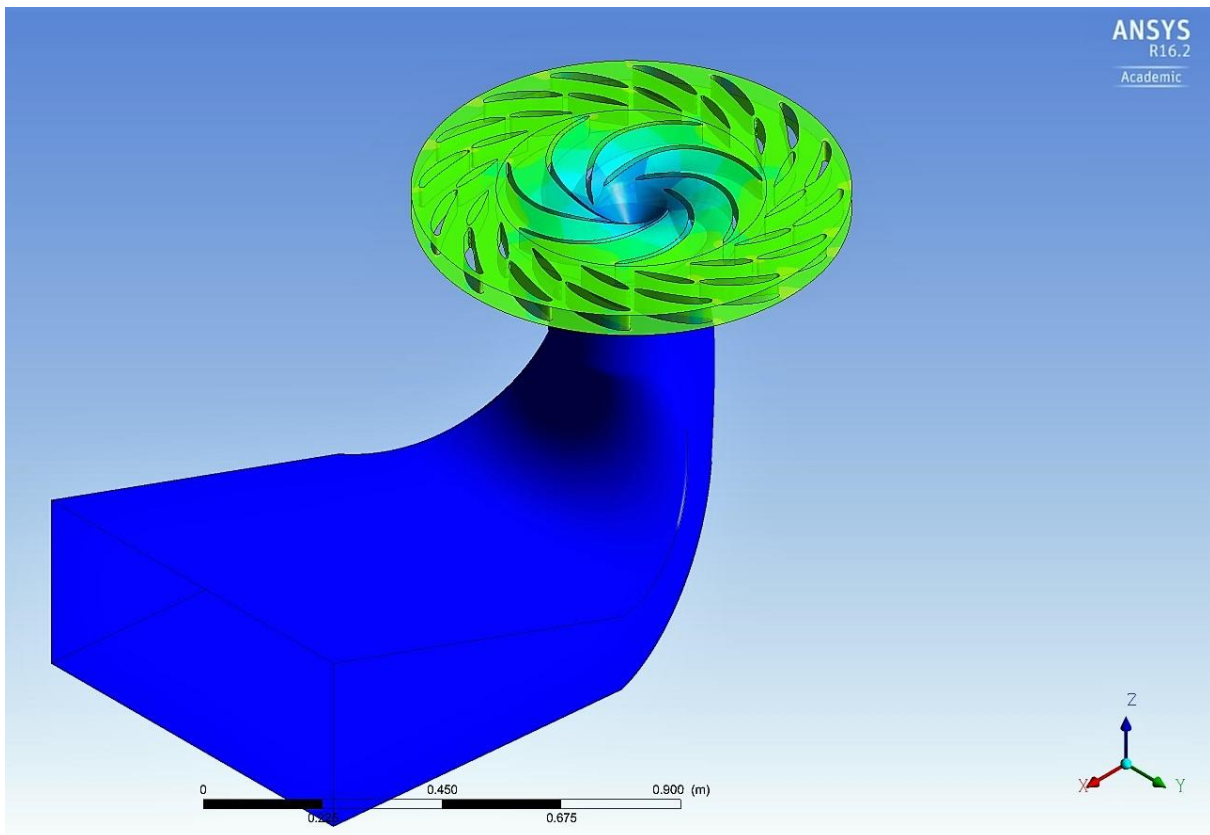


Figure 2. Computational model.

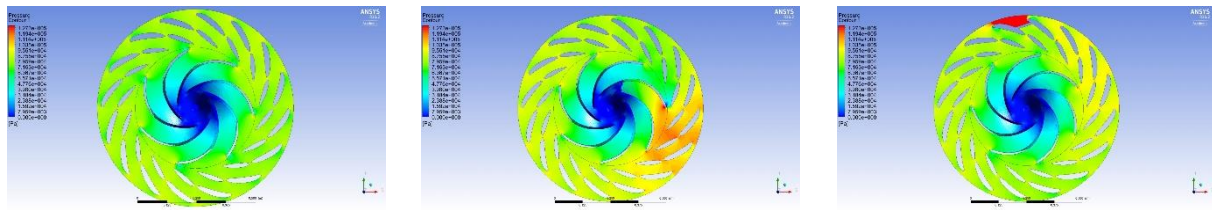
3. Results and discussion

3.1. Pressure contours

Figure 3 shows examples of the pressure contours obtained for the unobstructed turbine case and rotor/distribution blockage cases.

As it can be observed, a blockage in the rotor or the distributor of the machine creates a high-pressure region in the distributor. The difference between these two blockage cases is that in the case of a blockage rotor this high-pressure region travels through the distributor at a rotation speed equal to the

runner speed, while in the case of an obstructed distributor the high-pressure region remains confined to the distributor canal blocked.



Unobstructed turbine

50% obstructed rotor

100% obstructed distributor

Figure 3. Pressure contours obtained for studied cases.

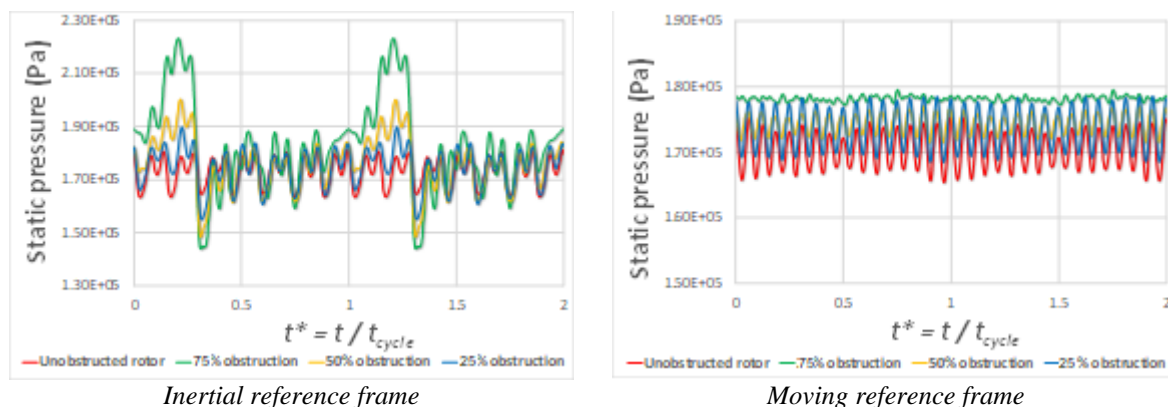
3.2. Obstructed rotor analysis

Figure 4 shows the pressure pulses obtained for different blockage sizes in a rotor canal, both for the inertial (distributor) and the moving (rotor) reference frame. A normalized time (t^*) was chosen for representation purposes ($t_{cycle} = \text{time for 1 full revolution} = 0.1 \text{ s}$).

It can be observed that for the inertial reference frame, the blockage amplifies the pressure pulse one time per rotation cycle. This is in concordance with the rotating high-pressure zone observed on the pressure contours. The amplitude of the pressure pulse is noticed to increase with blockage size.

In the moving reference frame, the most noticeable fact is that pressure values within the rotor are higher than those registered for the unobstructed case. For this case, the amplitude of the pressure pulse increases with the blockage size.

Figures 5 and 6 show the results obtained on the frequency domain. It can be noticed that while in the moving reference frame there is no substantial change in the excitation frequency, in the static reference frame the runner rotation frequency f_f and its harmonics take preponderance over the rotor blades frequency f_b .



Inertial reference frame

Moving reference frame

Figure 4. Pressure pulse signals for the obstructed rotor case.

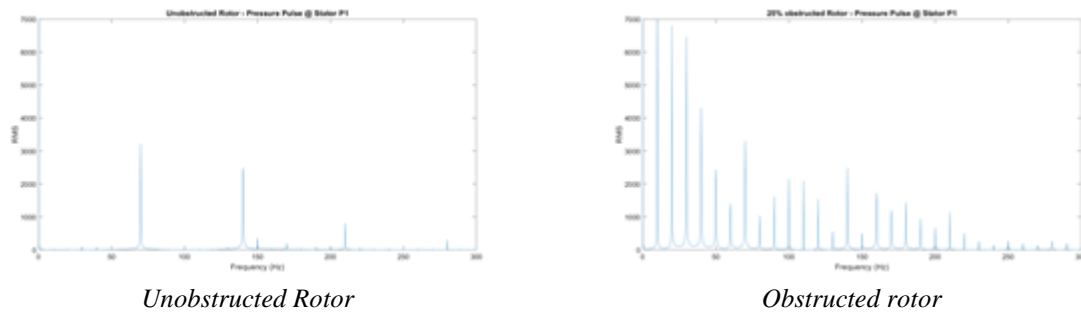


Figure 5. RSI frequencies in the static reference frame for obstructed rotor case.

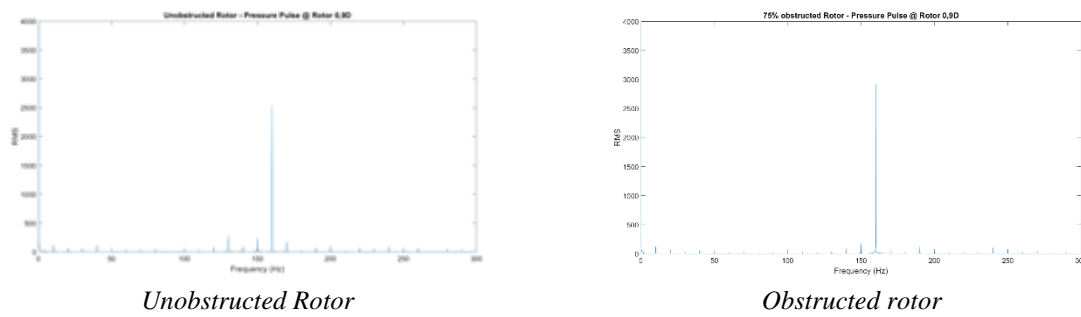


Figure 6. RSI frequencies in the rotating reference frame for obstructed rotor case.

3.3. *Obstructed distributor analysis*

Figure 7 shows the pressure pulses obtained for different blockage sizes in a distributor canal, both for the inertial (distributor) and the moving (rotor) reference frame. A normalized time was again chosen for representation purposes.

It can be observed that for the moving reference frame, the blockage amplifies the pressure pulse one time per rotation cycle. The amplitude of the pressure pulse is noticed to increase with blockage size. For this case, in the inertial reference frame the pressure pulse is unaltered but the pressure values increase with blockage size.

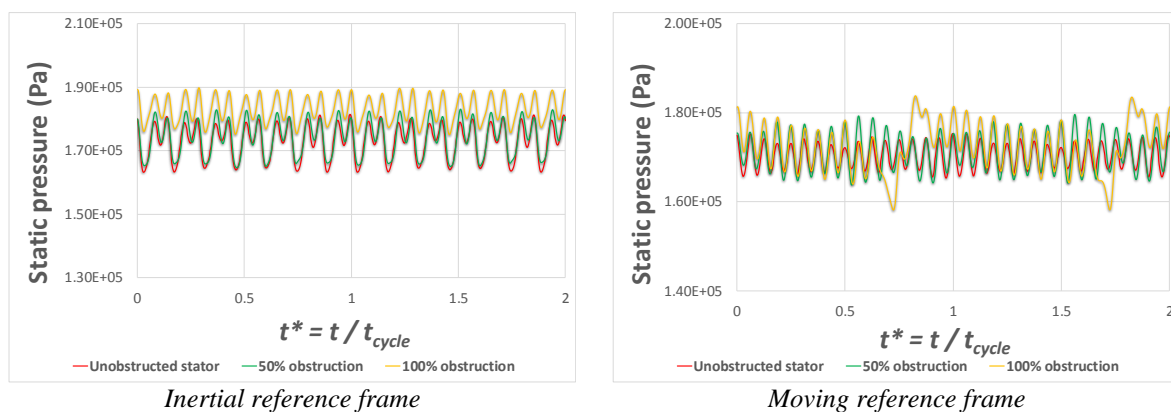


Figure 7. Pressure pulse signals for the obstructed distributor case.

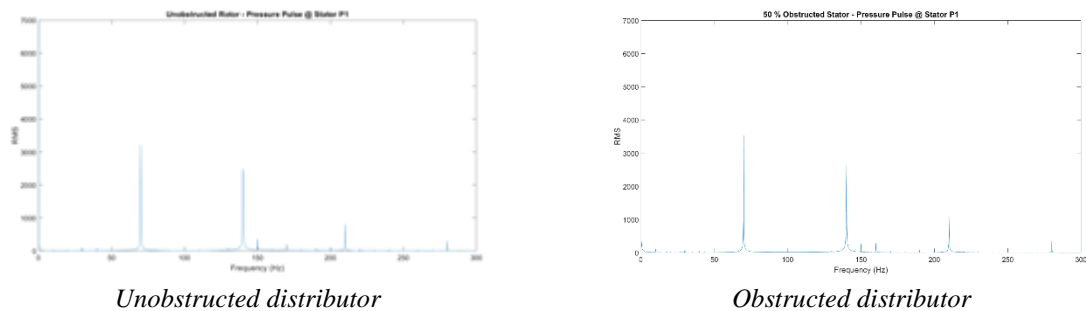


Figure 8. RSI frequencies in the static reference frame for obstructed rotor case.

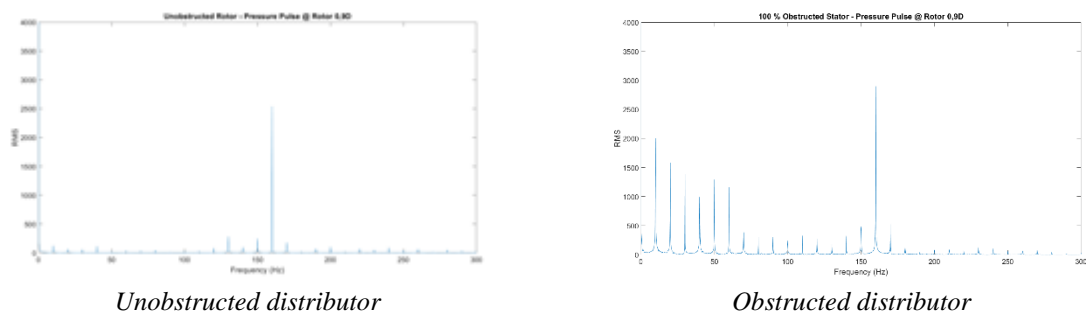


Figure 9. RSI frequencies in the rotating reference frame for obstructed rotor case.

Figures 8 and 9 show the results obtained on the frequency domain. It can be noticed that while in the static reference frame there is no substantial change in the excitation frequency, in the moving reference frame the runner rotation frequency f_f and its harmonics appear in the spectra.

4. Conclusions

Extraneous bodies may enter the hydraulic piping of hydropower plants. Generally, these bodies are broken parts of trash racks and stones detached from civil works (tunnels). In other cases, they are aspirated if the trash rack is broken.

Runner blockage reduces the efficiency of the turbine and generates an unbalanced radial hydraulic force. The effect of the blockage is considerable, as there is a significant increase in the pressure pulse even with a small blockage.

Blockage in the distributor affects the hydraulic pulsations and leads to a significant increase in the blade passing frequency amplitude. This means that the blockage increases the radial and axial dynamic forces on the runner.

References

- [1] Egusquiza E, de Paula L, 1994. Vibration diagnostic of a Francis Turbine. *17th IAHR Symposium on Hydraulic Machinery and Systems*, Beijing, China.
- [2] Egusquiza E, Escaler, X, Rosico E, 2002. Improving condition monitoring and diagnostics in

- hydromachinery. *Hydro Review Worldwide* 10 (November), 18 – 21.
- [3] Egusquiza E, Liang Q W, Escaler X, Valero C, 2006. Condition monitoring strategies in hydro powerplants. *1st International Conference on Hydropower Technology and Key Equipment*, Beijing, China.
- [4] Escaler X, Egusquiza E, Farhat M, Avellan F, Coussirat M, 2006. Detection of cavitation in hydraulic turbines. *Mechanical Systems and Signal Processing* 20, 983 – 1007.
- [5] Escaler X, Ekanger J V, Francke H H, Kjeldsen M, Nielsen T K, 2014. Detection of draft tube surge and erosive blade cavitation in a full-scale Francis turbine. *Jornal of Fluids Engineering* 137 (1), 011103
- [6] Egusquiza E, Valero C, Estévez A, Guardo A, Coussirat M, 2010. Failures due to ingested bodies in hydraulic turbines. *Engineering Failure Analysis* 18, 464 – 473.
- [7] Rodríguez C, Egusquiza E, Santos I, 2007. Frequencies in the vibration induced by the rotor stator interaction in a centrifugal pump turbine. *Journal of Fluids Engineering* 129, 1428 – 1435.
- [8] Menter F, 1993. Zonal two equation k- ω turbulence models for aerodynamic flows. *23rd Fluid Dynamics, Plasmadynamics and Lasers Conference*, Orlando FL, USA.